J. Asiat. Soc. Bangladesh, Sci. 40(2): 197-205, December 2014

SYNTHESIS OF NICKEL NANOPARTICLES USING POLY(VINYL ALCOHOL) AS A CAPPING AGENT

MOHAMMAD SHARIF HOSSAIN, MUHAMMED SHAH MIRAN, MD. ROKONUJJAMAN, MD. ABU BIN HASAN SUSAN, M. YOUSUF A. MOLLAH[1] AND M. M. RAHMAN[2]

Department of Chemistry, University of Dhaka, Dhaka 1000, Bangladesh

[2]University Grants Commission of Bangladesh, Agargaon, Dhaka1207, Bangladesh

Abstract

Nickel nanoparticles (NNPs) were synthesized by reduction of nickel (II) using poly(vinyl alcohol) (PVA) as a capping agent. The NNPs were characterized by transmission electron microscopy (TEM), scanning electron microscopy (SEM), energy dispersive X-ray (EDX) spectroscopy and X-ray diffraction (XRD) techniques. The addition of PVA has been found to profoundly influence the size, agglomeration and distribution of NNPs. The average diameters of NNPs are in the range of 3-7 nm in presence of PVA. XRD data indicate that NNPs are crystalline with face centered cubic structures. SEM images show the existence of secondary structures such as clusters and loops resulted from interactions between particles. The sizes of the NNPs were by and large uniform due to the use of PVA as the capping agent. FT-IR and thermogravimetric analyses confirm the interaction of PVA with NNPs to offer improved thermal stability.

Key words: Nanoparticles,Capping agent, PVA, Synthesis and morphology

Introduction

Ferro-magnetic elements like, nickel (Ni), iron (Fe) and cobalt (Co) have extensive applications in catalysis, solar energy absorption, permanent magnets, magnetic fluids and magnetic recording devices (Wang *et al.* 2002, Sun *et al.* 2001 and Pignard *et al.* 2000). Ni nano-structures are specifically important because of their potential applications in magnetic sensors and memory devices. Quite reasonably, last decade experienced extensive studies on synthesis and characterization of metal nanoparticles using a wide variety of methods which include: reverse micelle technique (Pileni 2003) and microemulsions (Hossain *et al.* 2012), chemical reduction of metal salts (Wang *et al.* 2000), electrochemical method (Yin *et al.* 2003 and Quayum *et al.* 2013), controlled decomposition of metastable organometallic compounds (Guan *et al.* 2002) and irradiation method (Esumi *et al.* 2003). ZnO (Ahmed *et al.* 2013, Sultana *et al.*, 2008) and ZnO@Ag core@shell NPs (Satter *et al.* 2014) have also been successfully prepared by using reverse micellar systems and water-in-oil microemulsions, respectively. However, extraction of NPs in solid phase from micellar core is difficult due to the possibility of agglomeration or aggregation. The use of a suitable capping agent therefore appears to be promising to prevent aggregation and conglomeration to tailor the sizes of NNPs. PVA, a water-soluble synthetic polymer with excellent film forming, emulsifying

[1] Corresponding author: Email: myamollah@hotmail.com

and adhesive properties, has recently been used as a capping agent (Patil *et al.* 2012, Khanna *et al.* 2005) for the preparation of silver (Ag) NPs.

In this study, we aimed at synthesizing NNPs through reduction of Ni(II) using PVA as a capping agent to tailor the size of NNPs within a narrow range. Primary objective was to develop a suitable method to synthesize nanosized nickel clusters in PVA matrix which is likely to serve as a stabilizer of nickel particles.

Materials and Methods

Chemicals: All the chemicals, nickel chloride hexahydrate ($NiCl_2.6H_2O$) (E. Merck, Germany), sodium borohydride ($NaBH_4$) (BDH Chemicals Ltd., England,) sodium hydroxide (NaOH) (E. Merck, Germany) and poly(vinyl alcohol) (PVA) (BDH Chemicals Ltd., England), were of analytical grades and used as received. Puric-S grade deionized water (Resistivity, R =2 ΩM/cm; Organo Co., Japan) prepared from distilled water was used to prepare solutions.

Preparation of Nickel Nanoparticles: A simple method of reduction in a confined matrix of PVA was used to synthesize NNPs. Colloidal $Ni(OH)_2$ was first prepared rapidly with stoichiometric addition of NaOH solution into an aqueous nickel chloride hexahydrate ($NiCl_2.6H_2O$) solution taken in a 100 mL glass beaker. Solution of PVA was mixed to the original solution separately. Stoichiometric excess of 0.5M $NaBH_4$ was added to the solution at 75°C to reduce $Ni(OH)_2$ into metallic nickel.

The mixture was kept under constant stirring for 2h at 75°C and turned dark black indicating the formation of nickel colloids. The mixture was then quickly transferred to an ice bath to quickly lower the temperature. The reduction reaction followed can be expressed as-

$$4Ni^{2+}(aq) + BH_4^-(aq) + 8OH^-(aq) \rightarrow 4Ni\,(s) + B(OH)_4^-(aq) + 4H_2O(l)$$

A portion of Ni/PVA solution was evaporated in a rotary evaporator. The highly dense Ni/PVA was completely dried by keeping the solution for 5 days at room temperature. The experiments were carried out with different concentrations of PVA in order to monitor the effect of concentration on the size and crystal structures of NNPs (Table 1).

Table 1. Preparation of nanocrystalline nickel in different molar ratios of nickel and PVA.

Sample no.	Volume of water (mL)	[PVA] (mmol)	[Ni^{2+}] (mmol)	[NaOH] (mmol)	[$NaBH_4$] (mmol)	Ni/PVA (molar ratio)
1	50	5.0	0.1	0.25	0.5	1:50
2	50	4.0	0.1	0.25	0.5	1:40
3	50	8.0	0.1	0.25	0.5	1:80

Characterization of NNPs: NNPs were characterized by TEM, SEM, EDX, FT-IR, TGA and XRD techniques. An FT-IR spectrometer (Shimadzu FT-IR IR-Prestige-21) was used for characterization of the NNPs and PVA to investigate the interaction between Ni and PVA. Calcium fluoride (CaF_2) crystal as windows was used for liquid samples to carry out FT-IR measurements for liquid samples. Thermogravimetric analysis (TGA-50, Shimadzu, Japan) of PVA and Ni/PVA samples were performed to check the thermal stability of PVA and Ni/PVA samples. Thermal stabilities were investigated at a heating rate of 10°C min^{-1} from ambient temperature to 580°C in an aluminum pan under nitrogen atmosphere. The XRD characterization of NNPs were carried out using a diffractometer (PAN analytical X' Pert PRO XRD PW 3040). The diffractometer used CuK_α radiation to analyze the phase composition with a wide range of Bragg angles, 2θ ranging from 0° to 90°. The SEM images of prepared NNPs were taken using S-3400N (Hitachi, Japan) for morphological analysis. EDX spectra were also recorded using S-3400N (Hitachi, Japan) to confirm the presence of elemental nickel. Particle size and morphology were further analysed by TEM (JEOL JEM-2011) equipped with a charge-couple device (CCD) camera (Gatan Inc.).

Results and Discussion

Interaction of PVA with nickel nanoparticles: Representative FT-IR spectra of the pure PVA and the NNPs with PVA are shown in Fig. 1.

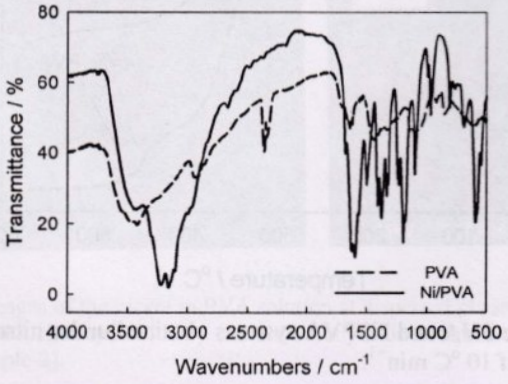

Fig. 1. FT-IR spectra of pure PVA and Ni/PVA solution.

The spectra show a strong and broad absorption at 3443 cm^{-1} for pure PVA and 3354 cm^{-1} for Ni-doped PVA. This band is assigned to O-H stretching vibration of hydroxyl group of PVA. The band corresponding to C-H asymmetric stretching vibration occurs at 2911 cm^{-1} and 2948 cm^{-1} for the PVA. The shifting and compression of this band is assigned to the interaction of the hydroxyl group with the positively charged surface of the NNPs (Duff *et al.* 1995). We suggest that stabilization of the NNPs may result mainly from the adsorption of the PVA chains on the particle surface, which are supposed to preferentially adsorb chloride ions at their outer surface (Duff *et al.* 1995) and also from the steric effect of the PVA polymer chain.

In addition, two new bands appeared in the range of 3250-3150 cm^{-1} Ni/PVA sample might be due to the interaction between Ni and PVA. This indicates that in spite of drying the sample may contain trace amount of water. The band at 1712 cm^{-1} corresponds to C=C stretching vibration and remains the same for Ni/PVA. Absorption at 1661 cm^{-1} corresponds to an acetyl C=O group, which may be explained on the basis of intra/inter molecular hydrogen bonding with the adjacent OH group. The sharp band at 1094 cm^{-1} corresponds to C-O stretching of acetyl groups present on the PVA backbone that shows a broad peak for Ni/PVA samples. An interaction between PVA and nickel is apparent.

Thermal stability of PVA in nickel nanoparticles: The thermal stability of PVA is likely to increase for Ni/PVA systems compared to pure PVA systems due to the interaction between Ni and PVA. To clarify thermal stability of pure PVA and Ni/PVA systems were analyzed by TGA (Fig. 2).

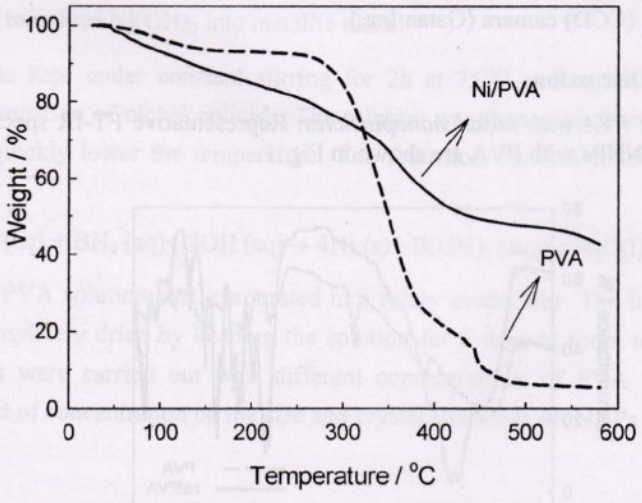

Fig. 2. TG curves of pure PVA and Ni/PVA systems obtained under nitrogen atmosphere at a heating rate of 10 °C min^{-1}.

The thermogram of pure PVA indicates three major stages of weight loss. In the first step, TG curves showed gradual weight loss (4%) due to the removal of free water up to around 110°C. In the second step, the PVA showed a steady weight loss (6%) between 110 and 280°C, which can be attributed to the elimination of low-molecular weight oligomers. Finally, in the third step, a sharp and gradual weight loss profile was observed starting at 290°C which represents the degradation of the skeletal chain structure of PVA. Above 480°C, the results obtained are associated with the residues only. There is also a significant hump observed at 444°C due to formation of an anhydride structure resulting from the decomposition of PVA at higher temperatures (Li *et al.* 2006 and El-Arnaouty and Eid 2010). The thermogram of Ni/PVA nanoparticles show four major events of weight loss. The first event occurring up to 130°C temperature is accompanied by a 10% weight loss and is related to the removal of the physically adsorbed water. In the second step 10% weight loss occurs from 130-260°C which might be due to the decomposition of inorganic substance present in PVA matrix. A gradual weight loss (6%) occurs in the temperature range 260-330°C, which corresponds to the elimination of oligomers. Finally the sharp decomposition of PVA occurs after degradation temperature at 334°C. The final step occurring in the 334-445°C temperature range with 24% weight loss indicates that total PVA is removed from the clusters and only nickel particles prevailed at higher temperatures. Careful analyses of TG thermograms indicate remarkable increase of degradation temperature of PVA from 290°C to 334°C with 6% weight loss. The thermal stability of PVA has thus been enhanced by NNPs.

Morphology and particle size distribution analyses by SEM and TEM: To analyze the morphology and structure of nickel nanoclusters in PVA matrix, SEM micrographs were taken in dispersed phase as shown in Fig. 3.

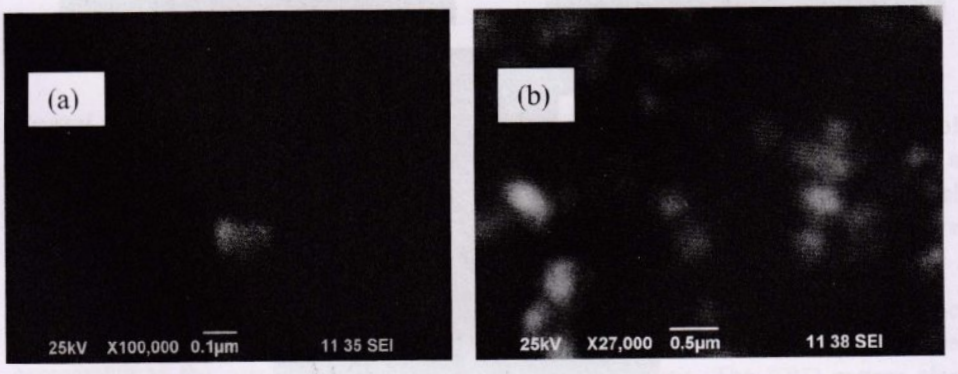

Fig. 3. SEM images of the nickel in PVA solution at dispersed phase obtained by the reduction of colloidal nickel hydroxide by sodium borohydride in aqueous medium [a = Sample-1 and b = sample-2].

SEM observation revealed the presence of crystalline particles in cluster form (Fig. 3.). The average cluster sizes were found to be 100 nm for Sample-1, where as it was around 200 nm for Sample 2 (Table 1). The NNPs prepared was nearly spherical in shape. The particles were agglomerated to form large clusters. This aggregation might have been resulted from magnetic interaction between the particles and polymer adherence (Duff *et al.* 1995).

Morphology of the obtained NNPs, were also characterized by TEM. Fig. 4 (a) shows a typical TEM image of Sample-1. The sizes of nickel clusters were averages from at least 400 particles. The average cluster size of Sample-1 was 2.7±0.6 nm with uniform size distribution. To the best of our knowledge, the obtained NNPs are one of the smallest Ni/PVA systems reported so far (Wang *et al.* 2005 and Guan *et al.* 2002). Figs. 4 (b) and (c) of Samples 2 and 3 respectively further revealed that the synthesized nickel particles were very small and uniform in size.

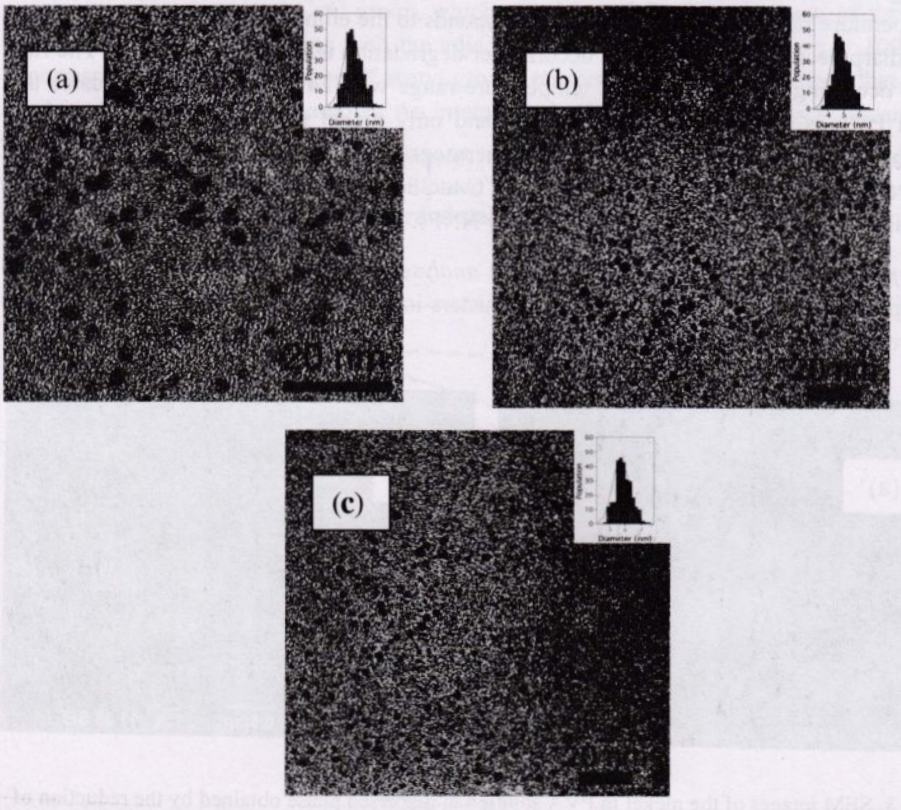

Fig. 4. TEM image of nickel prepared by reduction of nickel ions in PVA matrix and corresponding histograms (inset) of particle diameter [a = Sample-1, b = Sample-2, c = Sample-3].

Close analogy of TEM images indicated that most of the NNPs were quasi–spherical and their diameter was about 4.6±0.6 nm and 5.6±0.6 nm for Sample-2 and 3, respectively. It may, thus, be concluded that sizes and homogeneity of Ni NPs strongly depend on the concentration of PVA.

Elemental analysis of prepared nickel nanoclusters: For elemental analysis of the Ni/PVA nanoclusters an EDX spectrum of the dispersed phase was recorded (Fig. 5). The EDX spectrum reveals that the product contains nickel, carbon, oxygen, and sodium. Thus, it can be inferred that the NNPs co-exist with PVAs and salts of Na in solution (Eid *et al.* 2012).

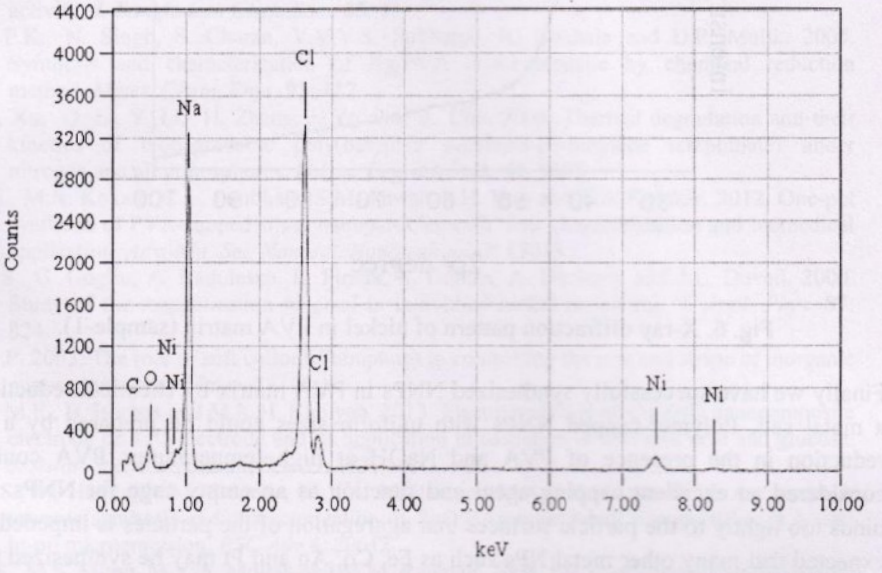

Fig. 5. EDX spectrum of the nickel in PVA solution (accelerating voltage: 20.0 keV).

Crystal structure of nickel nanoparticles: To study the influence of PVA on the size of nickel nanocrystals X-ray diffraction measurements were carried out for Sample-1 as a representative case. It can be illustrated from the X-ray data (Fig. 6) that the nickel nanoparticles are highly crystalline. The average crystallite sizes of these particles were calculated as 3.46 nm by using Scherrer formula.

It is well-known that crystallite size is different from particle size and a particle may be made up of several different crystallites. Particle sizes obtained by XRD analysis are comparable to the particle size estimated from TEM analysis. The XRD pattern also shows the feature of face centered cubic (fcc) nickel particles. The characteristic (100) plane of fcc nickel was observed at 41°. However, the characteristic peaks at (200) and (220) planes were absent in the diffractogram. This may be due to the interaction between

nickel and oxygen of PVA which may change the crystallographic orientations at these planes.

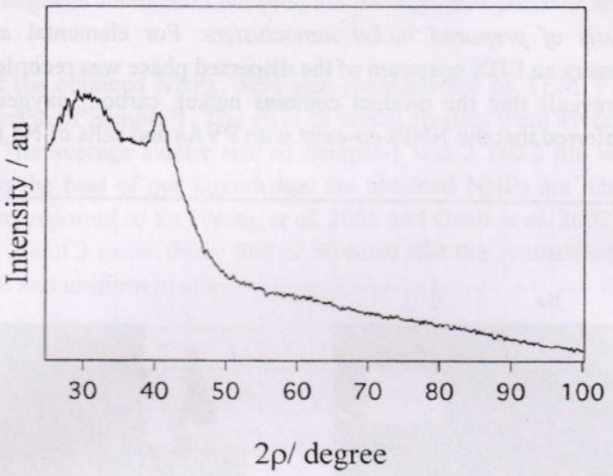

Fig. 6. X-ray diffraction pattern of nickel in PVA matrix (sample-1).

Finally we have successfully synthesized NNPs in PVA matrix by chemical reduction of a metal salt. Polymer-capped NNPs with uniform sizes could be prepared by a mild reduction in the presence of PVA and NaOH at high temperatures. PVA could be considered an excellent capping agent and function as an empty cage for NNPs. PVA binds too tightly to the particle surfaces that aggregation of the particles is impeded. It is expected that many other metal NPs such as Fe, Co, Au and Pt may be synthesized using PVA as the capping agent.

Acknowledgements

Analytical services from the Centre for Advanced Research in Sciences of University of Dhaka are gratefully acknowledged. FT-IR Spectral and TGA analyses were carried out by using equipment procured under a sub-project (CP-231) from Higher Education Quality Enhancement Project. The authors also acknowledge kind support from Instrumental Analysis Center of Yokohama National University, Japan for TEM measurements.

References

Ahmed, P., M.S. Miran, M.A.B.H. Susan and M.Y.A. Mollah. 2013. Growth process of zinc oxide nanoparticles in presence of reverse micelles of anionic and cationic surfactants. *J. Bangladesh Chem. Soc.* **26**: 20.

Duff, D.G., P.P. Edwards and B.F.G. Johnson. 1995. Formation of a polymer-protected platinum sol: a new understanding of the parameters controlling morphology. *J. Phys. Chem.* **99**: 15934.

El-Arnaouty, M.B.E. and M. Eid. 2010. Synthesis of grafted hydrogels as mono-divalent cation exchange for drug delivery. *Polym. Plast. Technol. Eng.* **49**: 182.

Esumi, K., K. Hayakawa and T. Yoshimura. 2003. Morphological change of gold-dendrimer nanocomposites by laser irradiation. *J. Colloid Interface Sci.* **268**: 501.

Guan, J.G.,W. Wang, R.Z. Gong, R.Z. Yuan, L.H. Gan and K.C. Tam. 2002. One-step synthesis of cobalt-phthalocyanine/iron nanocomposite particles with high magnetic susceptibility. *Langmuir*. **18**: 4198.

Hossain, S., U.K, Fatema, M.Y.A. Mollah, M.M. Rahman and M.A.B.H. Susan. 2012. Microemulsions as nanoreactors for preparation of nanoparticles with antibacterial activity. *J. Bangladesh Chem.Soc.*, **25**: 71.

Khanna, P.K., N. Singh, S. Charan, V.V.V.S. Subbarao, R. Gokhale and U.P. Mulik. 2005. Synthesis and characterization of Ag/PVA nanocomposite by chemical reduction method. *Mater. Chem. Phys.* **93**: 117.

Li, F., X. Xu, Q. Li, Y. Li, H. Zhang, J. Yu and A. Cao. 2006. Thermal degradation and their kinetics of biodegradable poly(butylene succinate-*co*-butylene terephthate) under nitrogen and air atmospheres. *Polym. Degrad. Stab.* **91**: 1685.

Patil, R.S., M.R. Kokate, C.L. Jambhale, S.M. Pawar, S.H. Han and S.S. Kolekar. 2012. One-pot synthesis of PVA-capped silver nanoparticles with their characterization and biomedical application. *Adv. Nat. Sci. Nanosci. Nanotechnol.* **3**: 15013.

Pignard, S., G. Goglio, A. Radulescu, L. Piraux, S. Dubois, A. Declemy and J.L. Duvail. 2000. Study of the magnetization reversal in individual nickel nanowires. *J. Appl. Phys.* **87**: 824.

Pileni, M.P. 2003. The role of soft colloidal templates in controlling the size and shape of inorganic nanocrystals. *Nat. Mater.* **2**: 145.

Quayum, M.E., B. Biswas and M.K.H. Bhuiyan. 2013. Electrosynthesis of Cu/ZnO nanocomposite electrode on ITO electrode and its application in oxidation of ascorbic acid and glucose. *J. Asiat. Soc. Bangladesh, Sci.* **39**: 183.

Satter, S.S., M. Hoque, M.M. Rahman, M.Y.A. Mollah and M.A.B.H. Susan. 2014. An approach towards synthesis and characterization of ZnO@Ag core@shell nanoparticles in water-in-oil microemulsion, *RSC Adv.***4**: 20612.

Sultana, S., M.S. Miran, M.Y.A. Mollah and M.M. Rahman. 2008. Effect of solvents on the growth kinetics of zinc oxide nanoparticles. *J. Bangladesh Chem. Soc.* **21**: 129.

Sun, L., P.C. Searson and C.L. Chien. 2001. Magnetic anisotropy in prismatic nickel nanowires. *Appl. Phys. Lett.* **79**: 4429.

Wang, Z.K., M.H. Kuok, S.C. Ng, D.J. Lockwood, M.G. Cottam, K. Nielsch, R.B. Wehrspohn and U. Gosele. 2002. Spin-wave quantization in ferromagnetic nickel nanowires. *Phys. Rev. B.* **89**: 027201.

Yin, B., H. Ma, S. Wang and S. Chen. 2003. Electrochemical synthesis of silver nanoparticles under protection of poly (*N*-vinylpyrrolidone). *J. Phys. Chem. B.* **107**: 8898.

(Received revised manuscript on 26 November 2014)